Using milling to explore physical states: The amorphous and polymorphic forms of sulindac

M. Latreche, J.F. Willart, M. Guerain, A. Hédoux, F. Danède

Univ. Lille, CNRS, INRA, ENSCL, UMR 8207
UMET - Unité Matériaux et Transformations
F-59000 Lille, France

Corresponding author: Jean-Francois.Willart@univ-lille1.fr

Abstract

This paper shows how milling can be used to explore the phase diagram of pharmaceuticals. This process has been applied to sulindac. A short milling has been found to trigger a polymorphic transformation between form II and form I upon heating which is not seen in the non-milled material. This possibility was clearly demonstrated to result from crystalline micro strains induced by the mechanical shocks. A long milling has been found to induce a total amorphization of the material. Moreover, the amorphous fraction produced during milling appears to have a complex recrystallization upon heating which depends on the milling time. The investigations have been mainly performed by differential scanning calorimetry and powder X-ray diffraction.

1. INTRODUCTION

Mechanical milling of powders is a usual process used in the course of drug formulation to reduce the particle size. However this process may also change the physical state of the end product[1-3], leading sometimes to an amorphization[4-10] and sometimes to a polymorphic transformation[11-15]. It appears, that amorphizations mainly occur when milling is performed below the glass transition temperature (Tg) of the material while polymorphic transformations mainly occur when milling is performed above Tg[13, 16, 17]. These transformations are expected to be governed by a competition between a mechanical disordering process and a thermally activated recrystallization. This competition explain that most materials only amorphize when they are milled below Tg since it is in the glass transition temperature range that the molecular mobility - which drives the crystallization - decreases the most rapidly. In some cases, the milling does not induce any apparent structural changes, but the microstructural changes it induces (size of crystallites, crystalline defects and lattice distortions) can strongly modify the physical stability of the material. This can lead for instance to polymorphic transformations upon heating[18] which do not occur in the non-milled crystal. Transformations induced by – or triggered by – milling have thus a strong repercussion on both the physical stability and the bioavailability of drugs[24]. That's why they have to be fully understood to be perfectly controlled[25, 26]. Moreover, they can also be used in a positive way to investigate further the phase diagram (polymorphism and relative stability of polymorphs) of pharmaceutical materials.

Sulindac (C_{20} H_{17} F O_3 S) is a nonsteroidal anti-inflammatory agent with a rich polymorphism. Three crystalline polymorphs were already reported: Forms I (CCDC number DOHREX01) and II (CCDC number DOHREX) which have respectively the space groups $P2_1/c$ [27] and *Pbca* [28], and form III whose structure has not yet been determined. The melting temperature and the melting enthalpy of form I have been found to be T_m^I = 187°C and ΔH_m^I = 66 J/g and those of form II has been found to be

T_m^{II} = 186°C and ΔH_m^{II} = 85 J/g. According to burgers' laws[29], since the highest melting point is associated to the lowest enthalpy of melting, form I and II are expected to form an enantiotropic system. This point, is also expected from the solubility curves of forms I and II in ethyl acetate which have been determined by Tung et al.[30] in the temperature range [6°C ; 54°C]. By extrapolation to higher temperatures, these curves are expected to cross around 160°C which suggests an inversion of the physical stability of forms II and I at this temperature. However, up to now, the transition between these two forms was never directly observed in the solid state suggesting that form II can be easily overheated above its expected transition temperature toward form I.

The objective of this paper is to investigate further the phase diagram of sulindac using original thermo-mechanical treatments. We will show, in particular, how the transition II→I can be easily triggered by a short milling process of form II and the causes of this triggering will be discussed in details. It will also be shown that a long milling leads to a total solid state amorphization of sulindac, which then shows a complex recrystallization pattern upon heating.

2. EXPERIMENTALS

Crystalline sulindac was provided by SIGMA® life science and used without any further purification.

Amorphous sulindac (quenched liquid) was prepared by heating (5°C/min) the above crystalline form in a DSC furnace up to the melting point, and by cooling (20°C/min) the melt to 20°C immediately after melting to avoid any potential thermal degradation. 100 mg of quenched liquid were thus produced by cumulating DSC heating batches of about 10 mg.

Ball milling was performed with a high energy planetary mill (Pulverisette 7 – Fritsch) using ZrO_2 milling jars of 43 cm^3 with seven balls (Ø=15 mm) of the same material. 1 g of sulindac powder was placed in the planetary mill corresponding to a ball:sample weight ratio of 75:1. The rotation speed of the solar disk was set to 400 rpm which corresponds to an average acceleration of the milling balls of 5 g (g = 9.81 ms^{-2} is the acceleration of gravity). We took care to alternate milling periods (typically 10 min) with pause periods (typically 5 min) in order to limit the mechanical heating of the sample.

Differential Scanning Calorimetry (DSC) experiments were performed with a Discovery micro calorimeter of TA Instruments. During all the measurements the calorimeter head was flushed with highly pure nitrogen gas. Temperature and enthalpy readings were calibrated using pure indium at the same scan rates used in the experiments. All DSC scans (heating and cooling) reported in the figures were performed at the rate of 5°C/min. The samples have been placed in open pans (pans with no lid) in order to allow any water absorbed during the milling process to evaporate upon heating. As recommended by the manufacturer small sample size (typically 4 mg) were used to achieve good resolution and good thermal conductivity.

Powder X-ray diffraction (PXRD) experiments were performed with a PanAlytical X'PERT PRO MPD diffractometer ($\lambda_{CuK\alpha}$ = 1.5418 Å for combined $K_{\alpha1}$ and $K_{\alpha2}$) equipped with an X'celerator detector (Almlo, The Netherlands). Samples were placed into Lindemann glass capillaries (Ø = 0.7mm) and installed on a rotating sample holder to avoid any artifacts due to preferential orientations of crystallites. Thermal treatments at a given temperature have been systematically carried out in the DSC device, using heating parameters identical to those used for the DSC investigations. All samples were thus heated at 5°C/min (or 0.5°C/min when specified) at a given temperature, annealed at this temperature for 15 min to allow any transformation to reach completion, and then cooled to 20°C at 20°C/min. The samples were then removed from the DSC pan, placed in a Lindeman capillary and analysed by PXRD. This protocol guaranties a very accurate control of the sample temperature and a perfect coherence between DSC and PXRD data. All X-ray diffraction patterns have thus been recorded at room temperature (RT), which has the advantage of avoiding any shift of Bragg peaks due to temperature changes and makes it possible the direct comparison of all diffraction patterns of the paper.

Thermogravimetric analysis (TGA) were performed with a Q500 TGA from TA Instruments (Guyancourt, France). Samples were placed in open aluminum pans, and the furnace was flushed with a highly pure nitrogen gas (50 mL/min). The temperature reading was calibrated using the Curie points of alumel and nickel, while the mass reading was calibrated using balance tare weights provided by TA Instruments. All TGA scans were performed at 5°C/min.

3. RESULTS AND DISCUSSION

3.1 Amorphization by melt quenching

Figure 1 shows the X-ray diffraction pattern of commercial sulindac (black line). It shows many sharp Bragg peaks indicating the crystalline character of the material. The position of these Bragg peaks corresponds to the polymorphic form II of sulindac characterized by the *orthorhombic Pbca* space group[28] [Koo and *al*. CSD: refcode DOHREX (code CCDC: 1143612)]. Figure 2 shows DSC heating scans (5°C/min) of commercial sulindac. Run 1 corresponds to the heating of the crystal. It only shows a well-defined endotherm at high temperature corresponding to the melting of form II. The melting temperature and the melting enthalpy are respectively T_m = 186°C and ΔH_m = 85 J/g. These values are consistent with those already reported in the literature[31]. The TGA scan (5°C/min) of the crystal is also reported in the insert of figure 2. It shows a noticeable loss of mass above 200°C corresponding to a chemical degradation of the material. This degradation occurs at least 10°C above the melting point so that sulindac can be safely melted provided that the melt be cooled immediately after the end of the melting process. Run 2 corresponds to the cooling (5°C/min) of the melt obtained after run 1. It does not show any signature of exothermic recrystallization which indicates that the liquid can be easily undercooled in the DSC at 5°C/min. Run 3 corresponds to the heating of the undercooled liquid. It shows a Cp jump (ΔCp = 0.40 J/g/°C) characteristic of a glass transition at Tg = 75°C. No exothermic recrystallization can be detected at higher temperatures. Sulindac thus appears to be a good glass former which is reluctant to recrystallization when heated with a moderate heating rate (5°C/min).

3.2 Amorphization by mechanical milling

The crystalline form II of sulindac has been milled in a planetary mill during 10 hours. The X-ray diffraction pattern of the milled material is reported in figure 1. It appears that the Bragg peaks characteristic of the initial crystalline form II have totally disappeared giving rise to a halo identical to that of the quenched liquid also reported in figure 1 for comparison. This strongly suggests that sulindac has undergone a solid state amorphization during the milling process. The heating DSC scan of the milled material is reported in figure 2 (run 4). It shows a Cp jump at Tg = 75°C characteristic of the glass transition of sulindac and at higher temperature a sharp recrystallization exotherm ranging from 95°C to 110°C. These two events indicate that a solid state amorphization of sulindac has occurred during the 10 hour milling and that the amorphous state thus obtained has a glassy character. Moreover, the amplitude of the Cp jump at Tg and the enthalpy of the recrystallization indicate that the amorphization is total. It must be noted that, for identical heating conditions, the amorphous state obtained upon milling recrystallizes unavoidably upon heating (run 4) while the quenched liquid does not (run 3). This reveals a greater physical stability of the quenched liquid over the amorphous state obtained by milling the crystal. The easier recrystallization of milling induced amorphous materials is a usual feature which can have different origins: (1) Remaining crystalline nuclei which have slipped through the milling[8, 9] can trigger the recrystallization process. (2) A different local order in the milled material can facilitate the recrystallization by changing the nucleation and growth properties of the crystalline form [10]. (3) The larger specific surface of the milled material can also promote the crystallization as molecular mobility is higher at the surface than in the bulk [18-20]. The X-ray diffraction pattern of the milled sample, recorded at room temperature after its recrystallization at 115°C is reported in figure 1. The recrystallization was achieved in the DSC device by heating (5°C/min) the milled materials up to 115°C, annealing at this temperature for 15 min and cooling (20°C/min) to 20°C (see section 2 for details). The diffractogram shows many well defined Bragg

peaks which are characteristic of the polymorphic form I of sulindac[27] (space group: monoclinic $P2_1/c$, CSD: refcode DOHREX01 (code CCDC: 637252)). No trace of the initial form II can be detected which indicates that the recrystallization of amorphous sulindac obtained by milling the crystal takes place entirely towards the form I.

The amorphization kinetics of sulindac upon milling has been investigated by PXRD and DSC. Figure 3a shows X-ray diffraction patterns recorded after different milling times, ranging from 0 to 10 hours. One can note a rapid decrease of the Bragg peak intensity accompanied by the development of an underlying broad halo which reflects the progressive amorphization of the material. The evolution is also marked by a strong broadening of the Bragg lines. This reflects a microstructural evolution of the remaining crystalline fraction which can be attributed to a strong crystallite size reduction and to the development of lattice strains upon milling. The disappearance of Bragg peaks is quite rapid so that after two hours of milling the milled material appears to be totally X-ray amorphous. No further modification of the PXRD pattern can be observed for longer milling times. Figure 3b presents the heating DSC scans (5°C/min) of sulindac recorded after different milling times, ranging from 0 to 10 hours. It shows the progressive development of an exothermic recrystallization which reflects the increasing amorphization with milling time. This recrystallization slightly shifts towards the high temperatures. It ranges from 75°C to 95°C after 5 min of milling while it ranges from 90°C to 105°C after 10 hours of milling. This shift reveals an increasing physical stability of the amorphized fraction as milling progresses. It can be due to an evolution of the structural short range order in the amorphized fractions during milling. We may think, in particular, that the short range order of freshly amorphized fractions shows a reminiscence of the initial crystalline order which progressively vanishes upon further milling. Such an evolution would make the recrystallization upon heating increasingly difficult. The shift of the recrystallization could also be due to the decrease in the number of remaining crystallites as milling progresses. These crystallites are likely to

facilitate the recrystallization of the amorphous fraction through a seeding effect, so that their gradual disappearance makes recrystallization more and more difficult.

The thermograms also show a Cp jump around 75°C whose amplitude increases in parallel with that of the enthalpy of recrystallization. It corresponds to the glass transition of the amorphized fraction. However, for short milling times, the Cp jump is truncated by the recrystallization exotherm which starts before the end of the glass transition. This effect is particularly pronounced for short milling times so that the glass transition cannot be clearly detected for milling times shorter than 10 minutes.

3.3 Recrystallization of milling induced amorphous sulindac

Figure 4, compares the PXRD patterns of sulindac recorded at RT after different milling times (in black) to those recorded after recrystallization at 120°C of the fraction amorphized by the milling (in blue). The recrystallization was achieved in the DSC device by heating (5°C/min) the milled materials up to 120°C, annealing at this temperature for 15 min and cooling (20°C/min) to 20°C (see section 2 for details). For short milling times (e.g. 5 min), after recrystallization, we note a strong enhancement of the intensity of Bragg peaks characteristic of form II and the apparition of tiny peaks of form I indicating that this latter form only exists in the state of traces. On the contrary, for long milling times (e.g. 600 min), the PXRD pattern of the recrystallized sample only shows the Bragg peaks of form I while those characteristic of form II cannot be detected. For intermediate milling times (e.g. 20 min) the PXRD pattern of the recrystallized sample shows both a noticeable enhancement of Bragg peaks corresponding to the initial form II and the clear development of Bragg peaks characteristic of form I. It thus appears that the recrystallization of the amorphized fraction upon heating is complex as both form I and II can develop in proportions which depend on the milling time. This recrystallization occurs toward form II for short milling times, toward form I for long milling times and toward a mixture of the two forms for intermediate milling times.

The recrystallization toward form II for short milling times could be due to a seeding effect of the amorphized fractions by the initial form II not yet amorphized by the milling. The latter disappears progressively during the milling so that the recrystallization is expected to be less and less oriented by the seeding effect. When the sample is totally amorphized, there are no more crystallites of form II and the recrystallization occurs entirely towards form I. The recrystallization toward form II could also be due to an evolution of the short range order of the amorphous fraction during milling. It is possible that the crystallites that have just been amorphized have a local order which exhibits a reminiscence of the crystalline order of the initial phase (form II) which could facilitate the recrystallization toward this phase. This reminiscent order is expected to progressively disappear upon further milling so that the recrystallization occurs no longer toward form II.

3.4 Polymorphic transition II→I upon heating

Interestingly, the thermograms recorded after short milling times (figure 3) show transiently an additional endotherm around 160°C which is not observed in the non-milled sulindac. It develops between 0 and 5 minutes of milling and then decreases for longer milling times to finally totally disappear after 60 minutes of milling. The origin of this peak has been investigated on the sample milled for 5 minutes for which the endotherm is maximum. Figure 5 shows X-ray diffraction patterns of this sample recorded at RT, just after milling and after heating at 120°C and 160°C (see section 2 for details). The black diffractogram has been recorded just after milling. It shows small Bragg peaks characteristic of form II superimposed to a broad diffuse bump. This indicates that the sample is a mixture of amorphous sulindac produced by the milling and remaining crystallites of form II. The red diffractogram has been recorded after heating (5°C/min) the sample at 120°C - i.e. just above the recrystallization exotherm (figure 3b) – annealing at this temperature for 15 minutes and cooling (20°C/min) to

20°C. It shows the decrease of the diffuse bump and a strong enhancement of the intensity of Bragg peaks of form II. Some tiny Bragg peaks characteristic of form I can however also be detected (e.g. at $2\theta = 10.85°$). The recrystallization thus appears to occur mainly toward form II. The blue diffractogram has been recorded after heating (5°C/min) the sample at 160°C, annealing at this temperature for 15 minutes and cooling (20°C/min) to 20°C. It shows a strong decrease of Bragg peaks characteristic of form II and a strong increase of those characteristic of form I. The endotherm around 160°C thus corresponds to a partial polymorphic transformation of form II toward form I. This is the first direct observation of this transition in sulindac, and its endothermic character definitely proves that forms I and II are enantiotropically related.

It must be noted that for milling longer than 5 minutes the endotherm at 160°C progressively disappears to finally vanishes after 60 minutes of milling. For this milling time, the sample is almost totally amorphous while the recrystallization upon heating still produces a significant amount of form II (figure 4). This indicates that the transition II→ I upon heating mainly concerns the fraction of form II not yet amorphized by the milling, and not that resulting from the recrystallization of the milling induced amorphous fraction.

One can also wonder why the transformation II→I occurs in the very shortly milled material while it is not detected in the absence of milling. Two main features distinguishing the milled and non-milled materials can be responsible for this difference. Upon heating, just before the transformation II→I, the material milled for 5 minutes is made of defective crystallites of form II not yet amorphized, mixed with non-defective crystallites of form I and II arising from the recrystallization of the amorphous fraction previously generated by the milling. On the contrary, the non-milled material is free of form I and crystallites of form II are not defective. These two essential differences suggest two possible scenarios which can trigger the transformation II→I upon heating:

- In the scenario 1, we might think that the traces of form I developing during the recrystallization of the milling induced amorphous fraction could act as seeds to trigger the transformation II→I at higher temperature. This could explain that the transformation does not occur in the non-milled material which is free of form I.

- In the scenario 2, the polymorphic transformation could be facilitated by the presence of crystalline defects in the milled form II which increases its Gibbs energy. It could also be promoted by the crystallite size reduction which increases the specific surface of the powder where nucleation and growth phenomena are known to be much faster than in the bulk[23].

To test the scenario 1, we have produced a sample made of non defective crystallites of form II seeded with crystallites of form I. This sample has been obtained in three steps: (1) Amorphous grains have been obtained by milling form II during 10 hours. (2) These amorphous grains have been mixed with non-milled crystallites of form II in the ratio [20:80]. (3) The mixture has then been heated (5°C/min) in the DSC device to induce both the wetting of form II by the amorphous fraction above Tg, and then the recrystallization of the amorphous fraction toward form I at higher temperature. Such a protocol makes the contact between forms I and II much better than in a simple physical mixture of the two crystalline forms. It is thus expected to enhance any potential seeding effect. The heating DSC scan of the seeded form II (run1) is reported in figure 6. It shows the effective recrystallization of the amorphous fraction between Tg and 110°C. Moreover, the diffractogram of the recrystallized sample recorded after heating the mixture up to 120°C is reported in figure 7a. It shows clearly the development of Bragg peaks characteristic of form I which confirms that the recrystallization has mainly occurred toward this form. At this point, the sample thus appears to be made of non-defective crystallites of form II seeded with crystallites of form I. However, upon further hating, the DSC run 1 of figure 6 does not reveal any sign of the polymorphic transformation around 160°C. Moreover, the X-ray diffraction

pattern recorded after heating the sample to 160°C (figure 7a) does not show any changes. These two results thus prove that a massive seeding of form II by form I does not trigger, by itself, the polymorphic transformation II→I.

To test the scenario 2, we have produced a sample made of strongly defective crystallites of form II without any crystallite of form I. Such a sample cannot be obtained simply by milling form II at RT as a noticeable amount of amourphous sulindac would be unavoidably produced. It has thus has been obtained by milling the crystalline form II at high temperature (130°C) for 5 minutes. This high temperature milling has been performed by equilibrating the milling jar containing the sample at 130°C in an external oven and then by milling the material at RT for 1 minute using the hot milling jar. The two previous steps were repeated 5 times to reach an effective milling time of 5 minutes at high temperature. The decrease of the milling jar temperature during the one minute milling stage at RT has been followed using an infrared thermometer. It appears that the temperature drop within one minute is about 3-5°C so that it can be estimated that the material has been milled at a temperature ranging between 125°C and 130°C. The DSC run 3 in figure 6 has been recorded after the 5 minute milling at high temperature. It does not show any trace of glass transition or any sign of exothermic recrystallization which indicates that the material does not contain any amorphous fraction after the high temperature milling. This behavior contrasts with that observed after the 5 minutes milling at RT where noticeable amorphization was detected (figure 3b). The absence of amorphization in the case of the high temperature milling is due to the fact the milling has been performed above the glass transition temperature of sulindac (Tg = 75°C). In this conditions, any amorphous fraction produced during the milling rapidly recrystallizes during the milling itself. Since this recrystallization involves tiny factions of amorphized sulindac, it is expected to occur toward form II as it is the case for sulindac shortly milled at RT (figure 4). This behavior is confirmed by the X-ray diffraction patterns of figure 7c recorded at RT just after the hot milling stage, which does not show any trace of form I. Hot milling was thus able to produce defective form

II not contaminated by form I nor by an amorphous fraction which could recrystallize toward form I upon heating. The DSC scans of figure 6 (runs 2 and 3) recorded after 2 and 5 minutes of milling at 130°C also show that the hot milled form II undergoes the polymorphic transformation II→I around 160°C. Moreover, the endotherm signaling the transformation increases with the milling time at high temperature indicating that the longer the milling the more complete the transformation II → I upon heating. This behavior is confirmed by the X-ray diffraction patterns of figures 7b and 7c recorded at RT after heating (5°C/min) the hot milled samples at 160°C - i.e. just above the II→I transformation – annealing at this temperature for 15 minutes and cooling (20°C/min) to 20°C. They show a strong increase of Bragg peaks characteristic of form I to the detriment of those characteristic of form II and this behavior appears to be all the more pronounced that that milling time is long. This clearly proves that the transformation II→I upon heating is triggered by the defects generated by the milling process.

Since the transformation II→ I is triggered by the damages induced by the mechanical chocks, the evolution of the microstructure of form II upon both milling and heating has been analyzed in details. Figure 8 shows the X-ray diffraction patterns of sulindac form II recorded before milling (in black) and just after a 10 minutes milling at 130°C (in red). Clearly, the Bragg peaks characteristic of form II (e.g. at 2θ = 9.67°) are broader after milling. This broadening generally reflects both a crystallite size reduction and / or the development of micro strains in the crystalline lattice. A detailed analysis of the diffractions lines by Rietveld refinement (comparison between a simulated diffraction pattern and the experimental one) has been performed using MAUD software[37] on each whole PXRD pattern (see ref [38] for more details). The diffractometer set-up contribution to broadening of the diffraction peaks has been determined using a NAC ($Na_2Ca_3Al_2F_{14}$) references provided by NIST. Such calculations allows the determination of the crystallite size and micro strains (local fluctuations of interreticular distances *d*, which can be expressed by $\varepsilon=\frac{\Delta d}{d}$) for each pattern. These data are reported in the insets of figure 8. They indicate that milling induces a strong decrease

of the average crystallite size d (d = 580 nm before milling and d = 60 nm after milling) and a strong increase of the lattice strains ε (ε = 0.0017 before milling and ε = 0.0038 after milling). Figure 8 also shows the X-ray diffraction patterns of milled sulindac recorded at RT after heating the milled sample at 160°C using a slow (0.5°C/min) and a fast (5°C/min) heating rate, annealing at this temperature for 15 minutes and cooling (20°C/min) to 20°C. In both cases, we observe an increase of the Bragg peaks characteristic of form I to the detriment of those characteristic of form II which signals the transformation of form II toward form I. However, this transformation is much stronger after the fast heating than after the slow one: 86% against 25% as derived from the analysis of the diffraction lines. Moreover, the Bragg peaks characteristic of the remaining hot milled form II (green and blue lines) after heating at 160°C are found to be much narrower than those recorded just after the milling process (red line). The average crystallite size and the micro strains derived from the analysis of the diffraction lines are reported in the inset of figure 8. It appears that the narrowing of Bragg peak of form II is mainly due to a strong decrease of the micro strains while the crystallite size is almost unchanged. This indicates that the micro strains in the milled crystal decreases during the heating stage and that this decrease is all the more pronounced that the heating rate is small and that the time spent at high temperature is long. The more or less partial character of the transformation must thus be attributed to the healing of crystal defects upon heating.

4. CONCLUSION

In this paper, we have studied the effects of milling on the structure of the crystalline form II of sulindac and on its evolutions upon subsequent heating. We have shown that, during milling, the fraction of crystalline form II decreases while that of amorphous sulindac increases so that a total amorphization occurs in less than 10 h of milling. Upon heating, the amorphous fraction recrystallizes toward forms I and II, the proportion of each form depending strongly on the milling duration. The longer the milling time, the larger the recrystallization toward form I. Interestingly, the crystalline fraction of form II not yet amorphized during the milling, undergoes a polymorphic transformation toward form I upon heating. Up to now, this transformation was never detected as it does not occur in the non-milled form II. This difference of behaviour illustrates how milling can reveal polymorphic transitions and thus clarify the phase diagram of pharmaceutical compounds. In the case of sulindac it proves that form I and II are enantiotropically related. We have also shown that the transition II→I upon heating is essentially triggered by the defects induced by the milling process and not by a seeding effect by form I resulting from the recrystallization of the amorphous fraction of sulindac unavoidably generated by the milling. This was made possible by preparing defective crystalline form II free of any amorphous fraction by high energy milling at high temperature (130°C, i.e. well above Tg).

ACKNOWLEDGEMENTS

This project has received funding from the Interreg 2 Seas programme 2014-2020 co-funded by the European Regional Development Fund under subsidy contract 2S01-059_IMODE

DATA AVAILABILITY

The raw/processed data used in this paper are not available on line.

CAPTIONS:

Figure 1: X-ray diffraction patterns of sulindac recorded at RT:

- form II non milled (black)
- form II milled 10 hours (green) in a planetary mill
- quenched liquid (blue)
- form II milled 10 hours and recrystallized at 115°C (red)

N.B.: Recrystallized samples were prepared in the DSC device. The samples were heated (5°C/min) up to 115°C, annealed at these temperatures for 15 minutes and cooled down to 20°C (20°C/min). See "Experimentals" section for details.

Figure 2: DSC scans (5°C/min) of sulindac:

- run 1: heating of the initial crystalline form II
- run 2: cooling of the melt
- run 3: heating of the quenched melt
- run 4 : heating of form II recorded after 10 h of milling in a planetary mill.

Insert: TGA scan (5°C/min) of crystalline form II.

Figure 3: X-ray diffraction patterns recorded at RT (a) and heating (5°C/min) DSC scans (b) of sulindac recorded after different milling times ranging from 0 to 600 min. The milling times are reported on the left hand side of each thermogram.

Figure 4: X-ray diffraction patterns of sulindac recorded at RT after different milling times as indicated on the left hand side of figure. The black patterns were recorded just after milling. The blue ones were recorded after recrystallization of amorphized fractions at 120°C. The recrystallization was achieved by heating (5°C/min) milled samples to 120°C, annealing at this

temperature for 15 min, and cooling (20°C/min) to 20°C. This thermal treatment was performed in the DSC device as explained in the "Experimentals" section.

Figure 5: X-ray diffraction patterns of sulindac recorded at RT after a 5 minute milling. The black curve was recorded just after milling. The red and blue curves were recorded after heating (5°C/min) the milled material to respectively 120°C and 160°C, annealing at these temperatures for 15 min, and cooling (20°C/min) to 20°C. This thermal treatment was performed in the DSC device as explained in the "Experimentals" section.

Figure 6: DSC heating scans (5°C/min) of sulindac:
Run 1 corresponds to a physical mixture made of 80 % of non-milled commercial crystalline sulindac (form II) and 20 % of amorphous sulindac previously obtained by a 10 hour milling process.
Run 2 and 3 correspond to commercial crystalline sulindac (form II) recorded after respectively 2 and 5 minutes of milling at 130°C (see text for details).

Figure 7: X-ray diffraction patterns of sulindac recorded at RT:
a) physical mixture made of 80 % of non-milled commercial crystalline sulindac (form II) and 20 % of amorphous sulindac previously obtained by a 10 hour milling process. The sample has been analyzed just after mixing and after heating to 120°C and 160°C.
b) and c) commercial crystalline sulindac (form II) milled respectively for 2 and 5 minutes at 130°C (see text for details). Each sample has been analyzed just after milling and after heating the milled material to 160°C.

N.B.: Thermal treatments were performed in the DSC device. The samples were heated (5°C/min) up to 120°C or 160°C, annealed at these temperatures for 15 minutes and cooled down to 20°C (20°C/min). See "Experimentals" section for details.

Figure 8: X-ray diffraction patterns of sulindac form II recorded at RT :

- (—): non-milled
- (—): milled for 10 minutes at 130°C
- (—): milled for 10 minutes at 130°C, and then heated from 20°C to 160°C at 0.5°C/min and cooled to 20°C at 20°C/min in the DSC device
- (—): milled for 10 minutes at 130 °C, and then heated from 20°C to 160°C at 5°C/min and cooled to 20°C at 20°C/min in the DSC device

The insets show the average crystallite sizes (d) and the lattice deformations (ε) of each sample derived from the analysis of the X-ray diffraction lines.

Figure 1

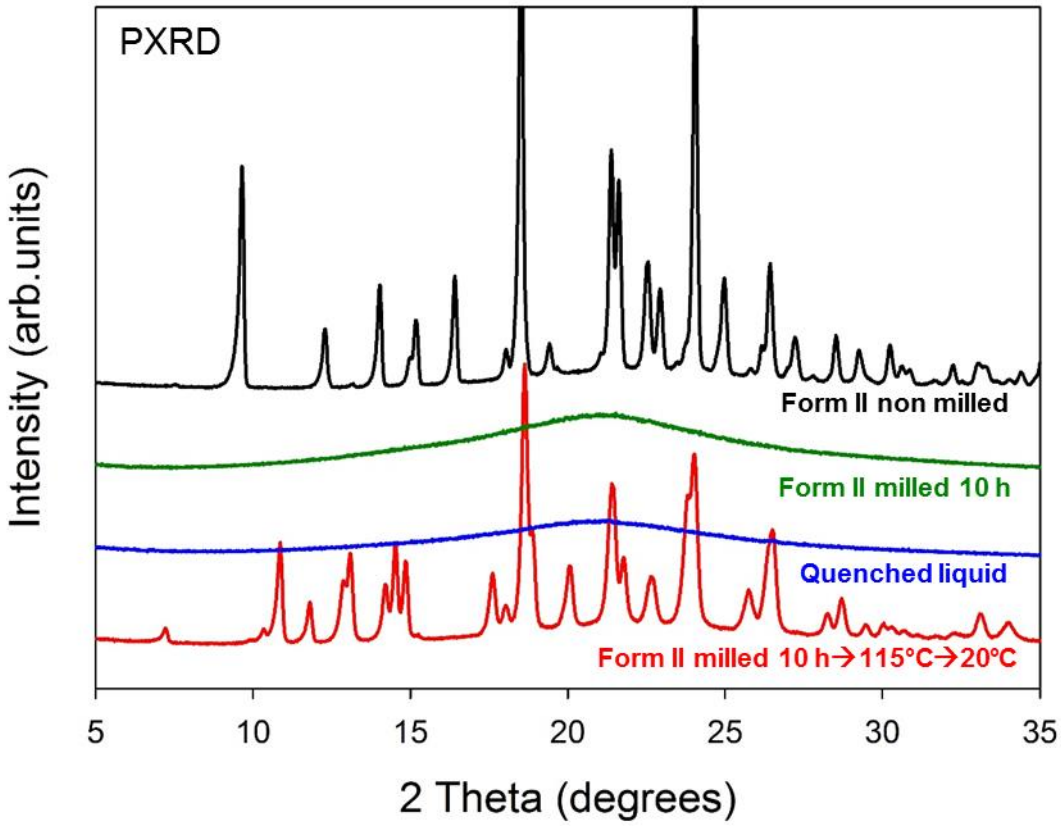
PXRD
Intensity (arb.units)
Form II non milled
Form II milled 10 h
Quenched liquid
Form II milled 10 h→115°C→20°C
5
10
15
20
25
30
35
2 Theta (degrees)

Figure 2

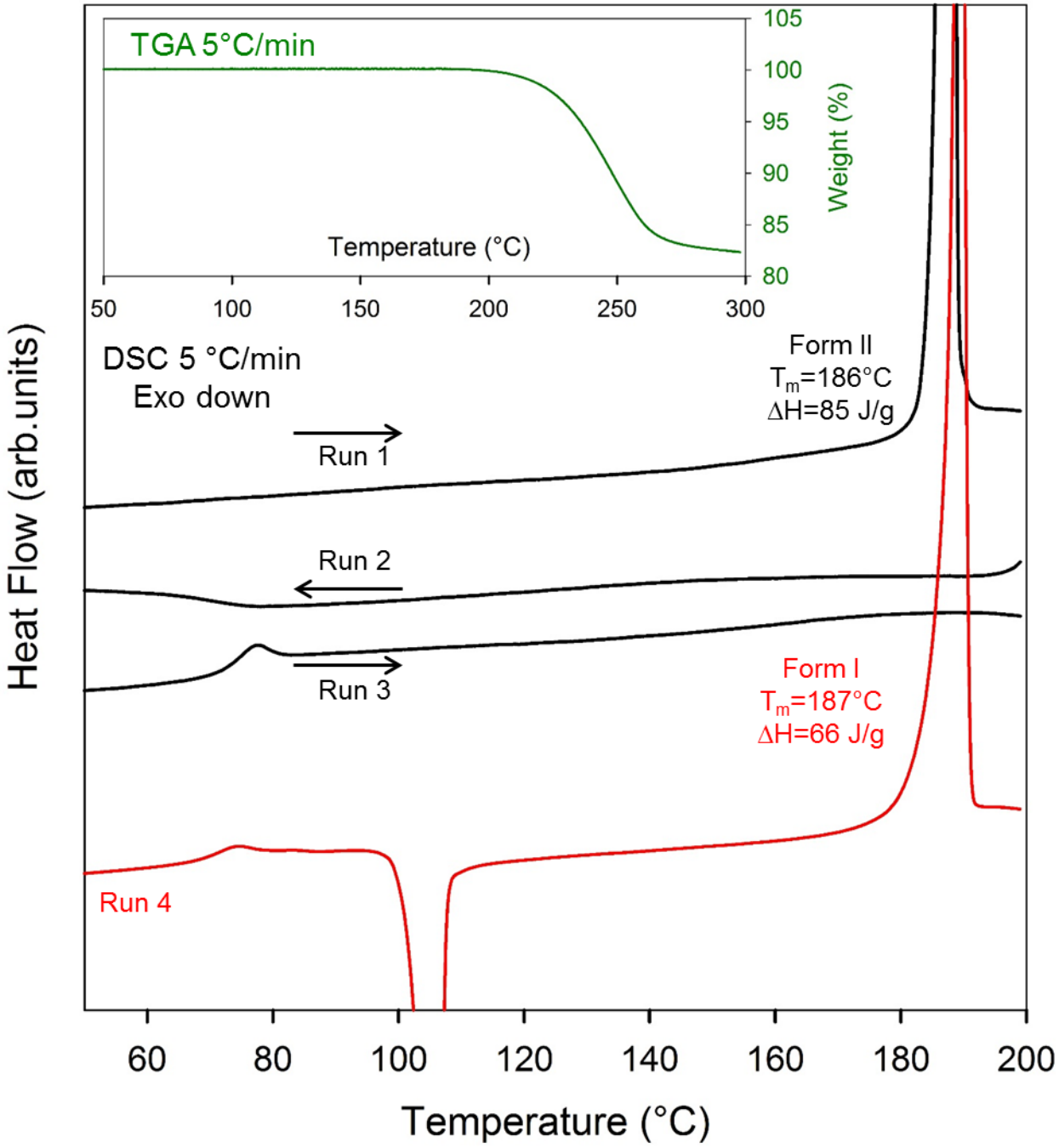
TGA 5°C/min
Temperature (°C)
Weight (%)
105
100
95
90
85
80
50
100
150
200
250
300
DSC 5 °C/min
Exo down
Form II
T_m=186°C
ΔH=85 J/g
Run 1
Run 2
Run 3
Form I
T_m=187°C
ΔH=66 J/g
Run 4
Heat Flow (arb.units)
60
80
100
120
140
160
180
200
Temperature (°C)

Figure 3

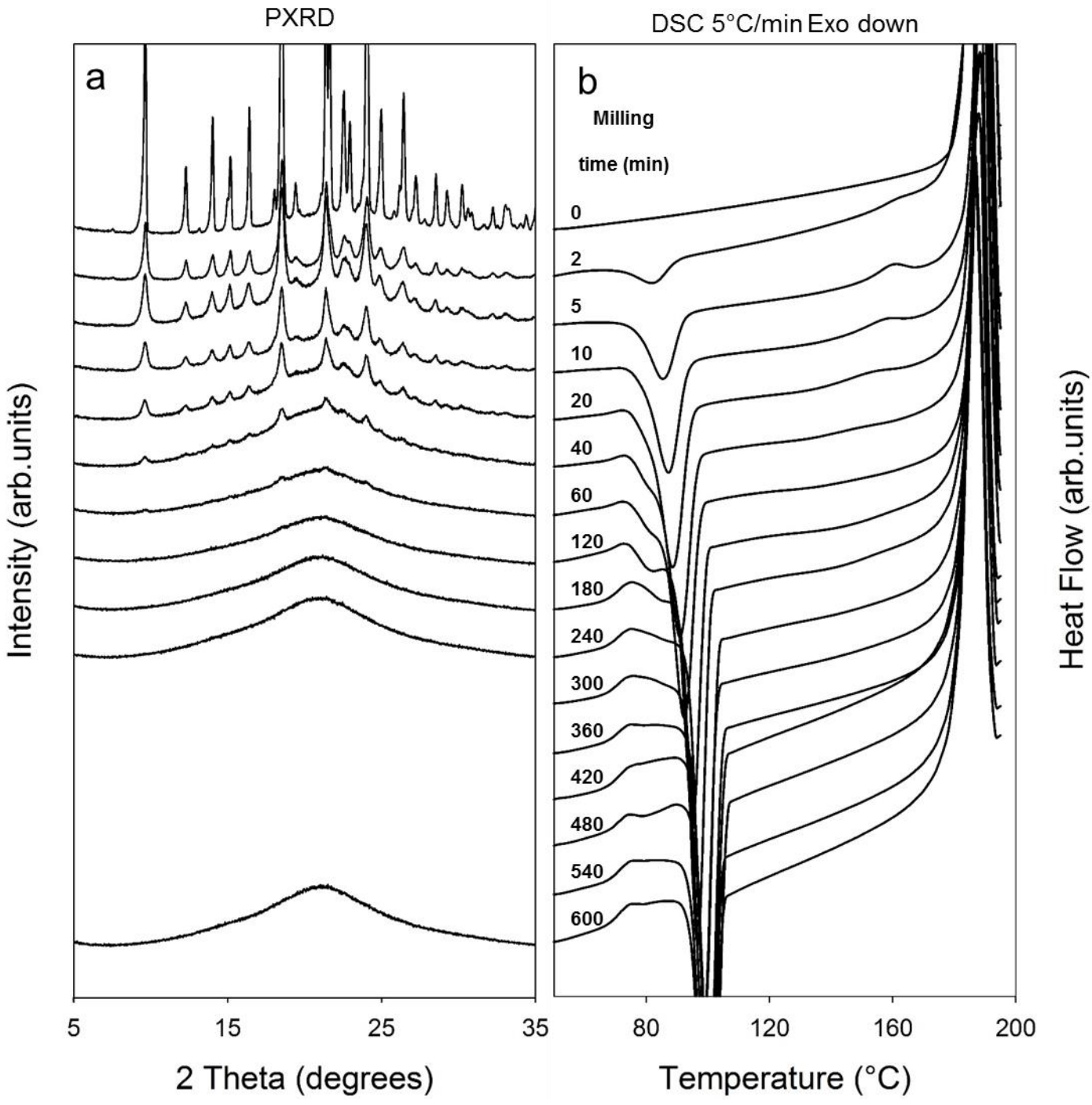
PXRD
DSC 5°C/min Exo down
a
b
Milling
time (min)
0
2
5
10
20
40
60
120
180
240
300
360
420
480
540
600
Intensity (arb.units)
Heat Flow (arb.units)
5
15
25
35
80
120
160
200
2 Theta (degrees)
Temperature (°C)

Figure 4

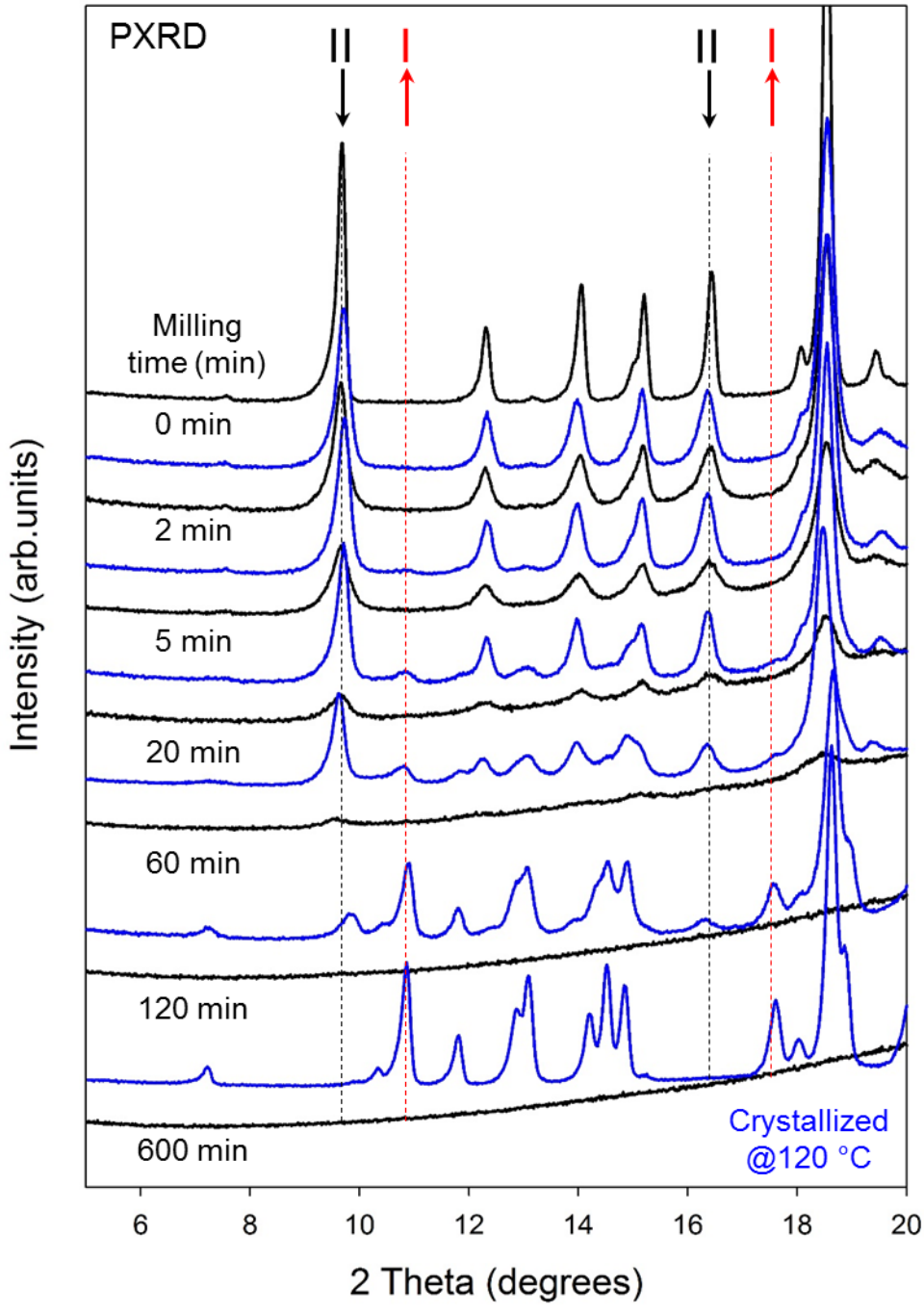
PXRD
II
I
II
I
Milling
time (min)
0 min
2 min
5 min
20 min
60 min
120 min
600 min
Crystallized
@120 °C
Intensity (arb.units)
6
8
10
12
14
16
18
20
2 Theta (degrees)

Figure 5

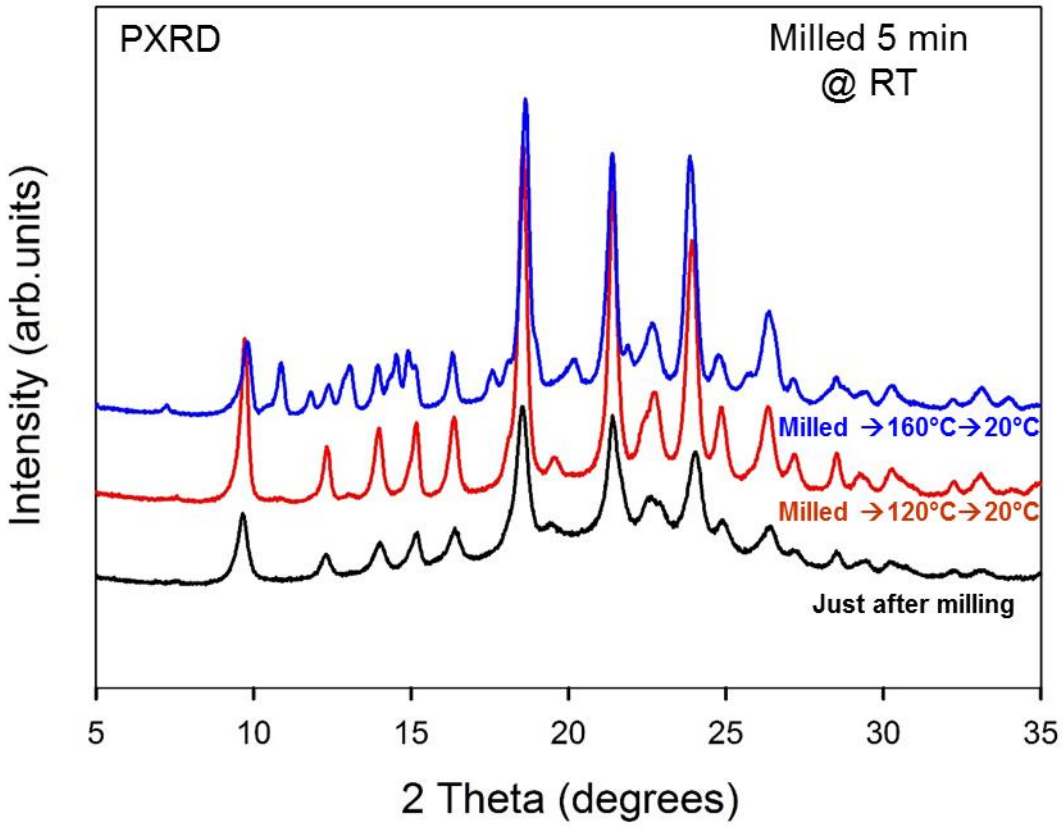
PXRD
Milled 5 min
@ RT
Intensity (arb.units)
Milled →160°C→20°C
Milled →120°C→20°C
Just after milling
5
10
15
20
25
30
35
2 Theta (degrees)

Figure 6

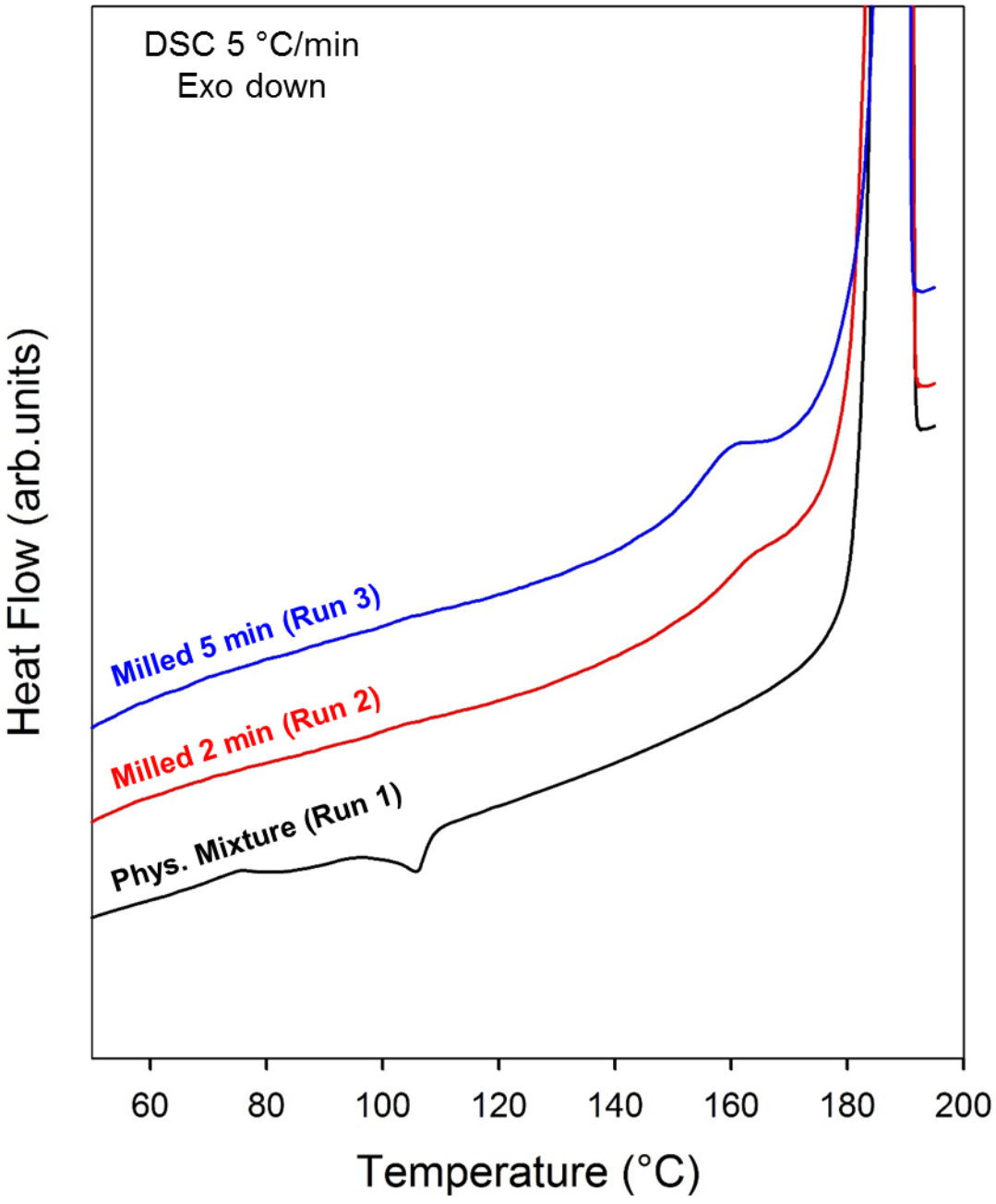
DSC 5 °C/min
Exo down
Heat Flow (arb.units)
Milled 5 min (Run 3)
Milled 2 min (Run 2)
Phys. Mixture (Run 1)
60
80
100
120
140
160
180
200
Temperature (°C)

Figure 7

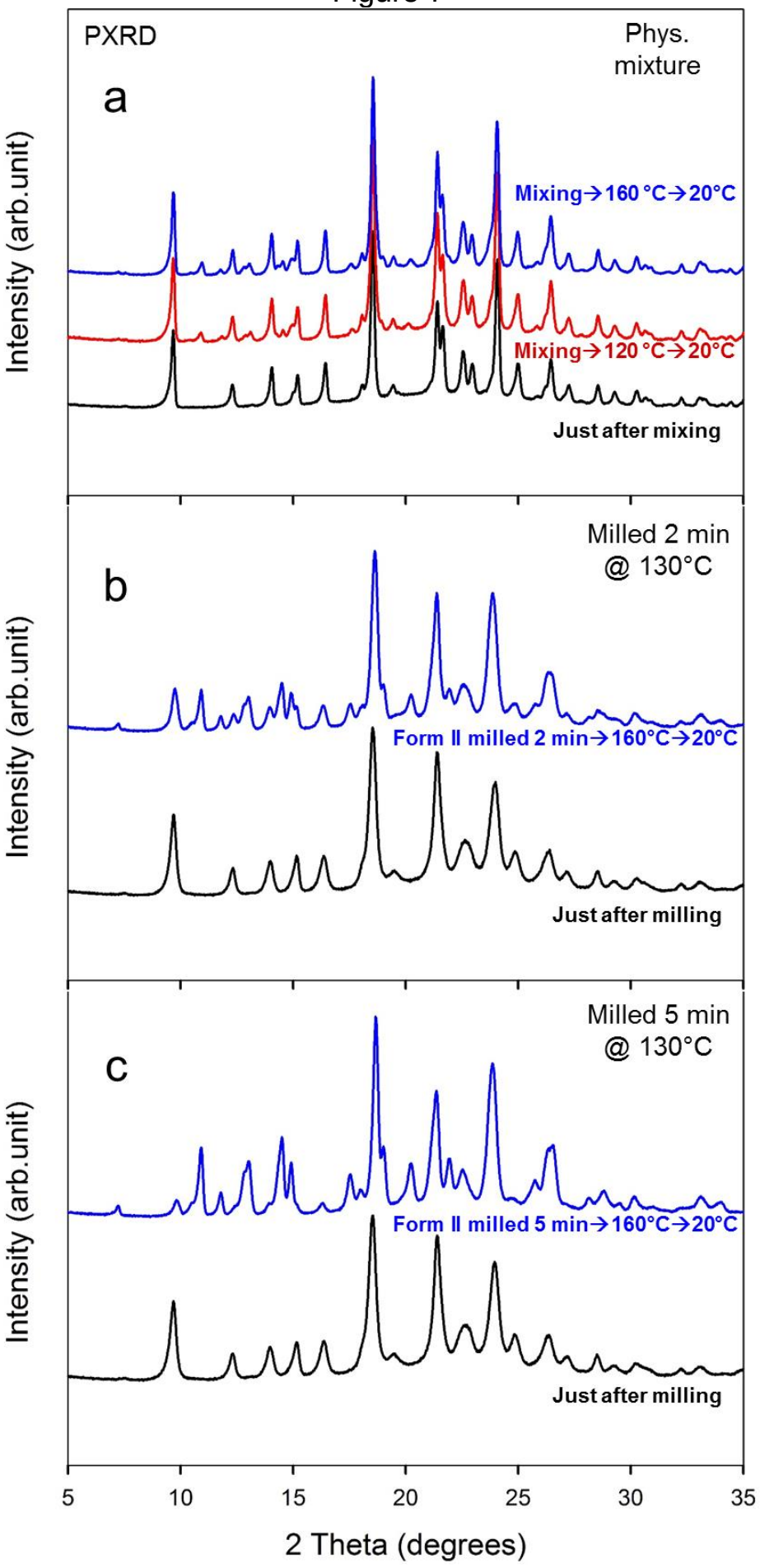
PXRD
Phys. mixture
a
Mixing→160 °C→20°C
Mixing→120 °C→20°C
Just after mixing
Intensity (arb.unit)
Milled 2 min @ 130°C
b
Form II milled 2 min→160°C→20°C
Just after milling
Intensity (arb.unit)
Milled 5 min @ 130°C
c
Form II milled 5 min→160°C→20°C
Just after milling
Intensity (arb.unit)
5
10
15
20
25
30
35
2 Theta (degrees)

Figure 8

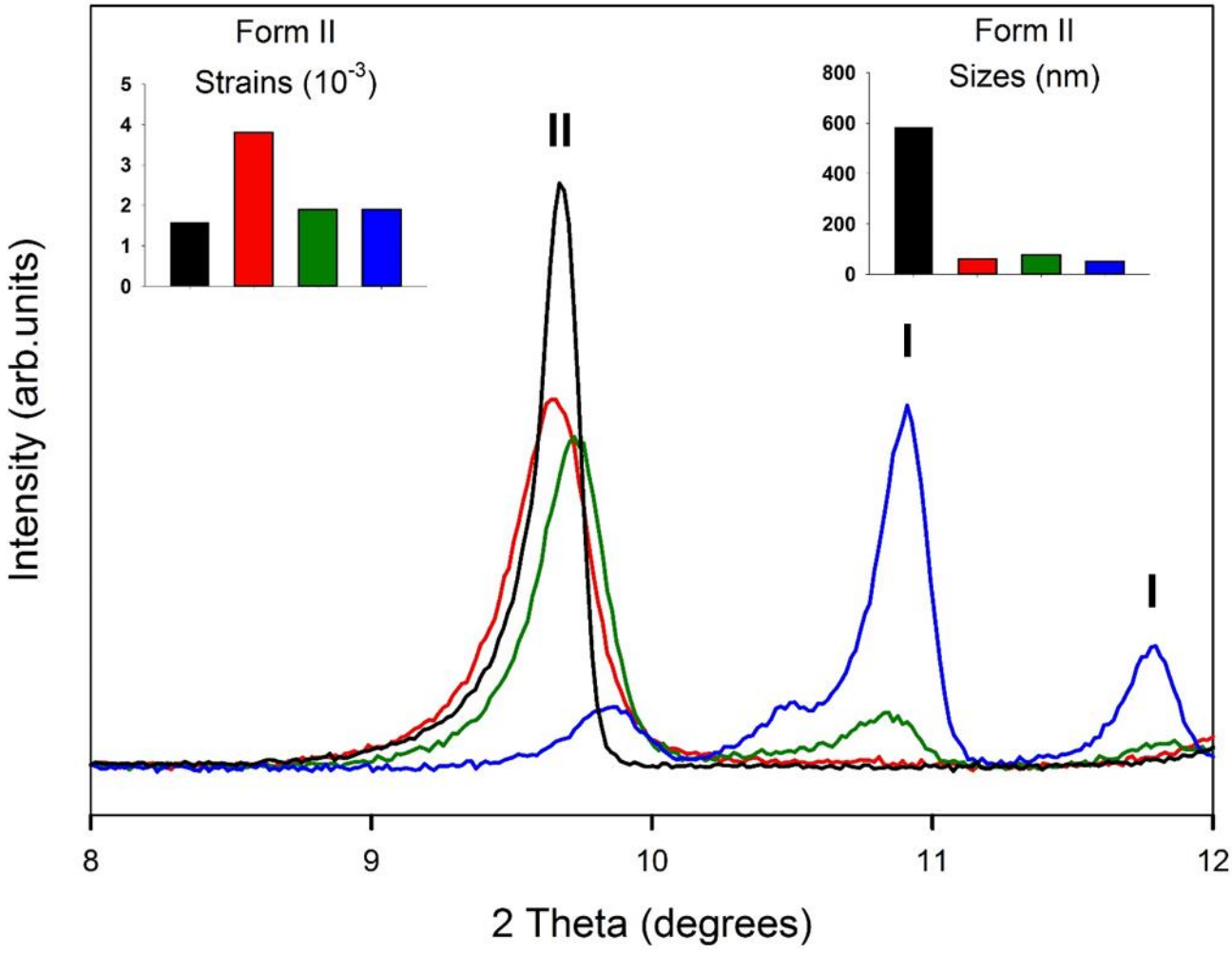
Form II
Strains (10^{-3})
5
4
3
2
1
0
Form II
Sizes (nm)
800
600
400
200
0
II
I
I
Intensity (arb.units)
8
9
10
11
12
2 Theta (degrees)

REFERENCES

1 J. F. Willart and M. Descamps, *Solid State Amorphization of Pharmaceuticals*, Molecular Pharmaceutics **5**, 905 (2008)

2 H. G. Brittain, *Effects of mechanical processing on phase composition*, Journal of Pharmaceutical Sciences **91**, 1573 (2002)

3 M. Descamps and J. F. Willart, *Perspectives on the amorphisation/milling relationship in pharmaceutical materials*, Advanced Drug Delivery Reviews **100**, 51 (2016)

4 P. Bordet, A. Bytchkov, M. Descamps, E. Dudognon, E. Elkaïm, P. Martinetto, W. Pagnoux, A. Poulain, and J. F. Willart, *Solid State Amorphization of β-Trehalose: A Structural Investigation Using Synchrotron Powder Diffraction and PDF Analysis*, Crystal Growth and Design **16**, 4547 (2016)

5 N. Dujardin, J. Willart, E. Dudognon, A. Hedoux, Y. Guinet, L. Paccou, B. Chazallon, and M. Descamps, *Solid state vitrification of crystalline α and β-D-glucose by mechanical milling*, Solid State Communications **148**, 78 (2008)

6 J. F. Willart, M. Durand, L. E. Briggner, A. Marx, F. Danède, and M. Descamps, *Solid-state amorphization of linaprazan by mechanical milling and evidence of polymorphism*, Journal of Pharmaceutical Sciences **102**, 2214 (2013)

7 B. Schammé, N. Couvrat, P. Malpeli, E. Dudognon, L. Delbreilh, V. Dupray, É. Dargent, and G. Coquerel, *Transformation of an active pharmaceutical ingredient upon high-energy milling: A process-induced disorder in Biclotymol*, International Journal of Pharmaceutics **499**, 67 (2016)

8 S. Qi, I. Weuts, S. De Cort, S. Stokbroekx, R. Leemans, M. Reading, P. Belton, and D. Q. M. Craig, *An investigation into the crystallisation behaviour of an amorphous cryomilled pharmaceutical material above and below the glass transition temperature*, Journal of Pharmaceutical Sciences **99**, 196 (2010)

9 N. Chieng, T. Rades, and D. Saville, *Formation and physical stability of the amorphous phase of ranitidine hydrochloride polymorphs prepared by cryo-milling*, European Journal of Pharmaceutics and Biopharmaceutics **68**, 771 (2008)

10 N. S. Trasi and S. R. Byrn, *Mechanically Induced Amorphization of Drugs: A Study of the Thermal Behavior of Cryomilled Compounds*, AAPS PharmSciTech **13**, 772 (2012)

11 P. Martinetto, P. Bordet, M. Descamps, E. Dudognon, W. Pagnoux, and J.-F. Willart, *Structural Transformations of d-Mannitol Induced by in Situ Milling Using Real Time Powder Synchrotron Radiation Diffraction*, Crystal Growth & Design **17**, 6111 (2017)

12 J. Willart, J. Lefebvre, F. Danede, S. Comini, P. Looten, and M. Descamps, *Polymorphic transformation of the Γ-form of -sorbitol upon milling: structural and nanostructural analyses*, Solid State Communications **135**, 519 (2005)

13 A. De Gusseme, C. Neves, J. F. Willart, A. Rameau, and M. Descamps, *Ordering and disordering of molecular solids upon mechanical milling: The case of fananserine*, Journal of Pharmaceutical Sciences **97**, 5000 (2008)

14 M. Matsuoka, J. Hirata, and S. Yoshizawa, *Kinetics of solid-state polymorphic transition of glycine in mechano-chemical processing*, Chemical Engineering Research and Design **88**, 1169 (2010)

15 H. G. Brittain, *Polymorphism and solvatomorphism 2010*, Journal of Pharmaceutical Sciences **101**, 464 (2012)

16 M. Descamps, J. F. Willart, E. Dudognon, and V. Caron, *Transformation of pharmaceutical compounds upon milling and comilling: The role ofTg*, Journal of Pharmaceutical Sciences **96**, 1398 (2007)

17 N. Chieng, Z. Zujovic, G. Bowmaker, T. Rades, and D. Saville, *Effect of milling conditions on the solid-state conversion of ranitidine hydrochloride form 1*, International Journal of Pharmaceutics **327**, 36 (2006)
18 P. F. M. Oliveira, J.-F. Willart, J. Siepmann, F. Siepmann, and M. Descamps, *Using Milling To Explore Physical States: The Amorphous and Polymorphic Forms of Dexamethasone*, Crystal Growth & Design **18**, 1748 (2018)
19 S. Desprez and M. Descamps, *Transformations of glassy indomethacin induced by ball-milling*, Journal of Non-Crystalline Solids **352**, 4480 (2006)
20 S. Chattoraj, C. Bhugra, C. Telang, L. Zhong, Z. Wang, and C. C. Sun, *Origin of Two Modes of Non-isothermal Crystallization of Glasses Produced by Milling*, Pharmaceutical Research, 1 (2011)
21 J.-F. Willart, L. Carpentier, F. Danède, and M. Descamps, *Solid-state vitrification of crystalline griseofulvin by mechanical milling*, Journal of Pharmaceutical Sciences **101**, 1570 (2012)
22 M. Hasebe, D. Musumeci, and L. Yu, *Fast surface crystallization of molecular glasses: creation of depletion zones by surface diffusion and crystallization flux*, J Phys Chem B **119**, 3304 (2015)
23 L. Yu, *Surface mobility of molecular glasses and its importance in physical stability*, Advanced Drug Delivery Reviews **100**, 3 (2016)
24 H. G. Brittain and D. J. W. Grant, in *Polymorphism in Pharmaceutical Sciences, Drugs and the Pharmaceutical Sciences*, edited by H. G. Brittain (Marcel Dekker, New York, 1999), Vol. 95, p. 279.
25 E. Shalaev, M. Shalaeva, and G. Zografi, *The effect of disorder on the chemical reactivity of an organic solid, tetraglycine methyl ester: Change of the reaction mechanism*, Journal of Pharmaceutical Sciences **91**, 584 (2002)
26 S. Qi, in *Disordered Pharmaceutical Materials* (Wiley-VCH Verlag GmbH & Co. KGaA, 2016), p. 467.
27 A. Llinas, K. J. Box, J. C. Burley, R. C. Glen, and J. M. Goodman, *A new method for the reproducible generation of polymorphs: two forms of sulindac with very different solubilities*, Journal of Applied Crystallography **40**, 379 (2007)
28 Chung Hoe Koo, Sang Hern Kim, and Wanchui Shin, *Crystal Structure of Antiinflammatory Sulindac*, Bulletin of the Korean Chemical Society **6**, 222 (1985)
29 A. Burger and R. Ramberger, *On the polymorphism of pharmaceuticals and other molecular crystals. I. Theory of thermodynamic rules*, Mikrochimica Acta **II**, 259 (1979)
30 H. H. Tung, E. L. Paul, M. Midler, and J. A. McCauley, *Crystallization of Organic Compounds: An Industrial Perspective* (Wiley, 2009).
31 R. B. Guerra, D. A. Gálico, and B. B. C. Holanda, *A new method for the reproducible generation of polymorphs: two forms of sulindac with very different solubilities*, J Therm Anal Calorim **123**, 2523 (2016)
32 R. Lefort, A. De Gusseme, J. F. Willart, F. Danède, and M. Descamps, *Solid state NMR and DSC methods for quantifying the amorphous content in solid dosage forms: an application to ball-milling of trehalose*, International Journal of Pharmaceutics **280**, 209 (2004)
33 J. F. Willart, E. Dudognon, A. Mahieu, M. Eddleston, W. Jones, and M. Descamps, *The role of cracks in the crystal nucleation process of amorphous griseofulvin*, European Physical Journal: Special Topics **226**, 837 (2017)
34 M. Descamps and E. Dudognon, *Crystallization from the amorphous state: Nucleation-growth decoupling, polymorphism interplay, and the role of interfaces*, Journal of Pharmaceutical Sciences **103**, 2615 (2014)

35 L. Zhu, L. Wong, and L. Yu, *Surface-Enhanced Crystallization of Amorphous Nifedipine*, Molecular Pharmaceutics **5**, 921 (2008)
36 S. Chen, H. Xi, and L. Yu, *Cross-Nucleation between ROY Polymorphs*, Journal of the American Chemical Society **127**, 17439 (2005)
37 R. A. Young, *The Rietveld Method* (Oxford University Press, 1995).
38 L. Lutterotti, *Total pattern fitting for the combined size–strain–stress–texture determination in thin film diffraction*, Nuclear Instruments and Methods in Physics Research Section B: Beam Interactions with Materials and Atoms **268**, 334 (2010)